Inorganic Chemistry

Article

pubs.acs.org/IC

Magnetic Orderings in $Li_2Cu(WO_4)_2$ with Tungstate-Bridged Quasi-1D Spin-1/2 Chains

I. Panneer Muthuselvam,[†,‡] Raman Sankar,[†] Viveka Nand Singh,[¶,§] G. Narsinga Rao,[†] Wei-Li Lee,[‡] Guang-Yu Guo,*[,§] and Fang-Cheng Chou*[,†,∥,⊥]

[†]Center for Condensed Matter Sciences and [§]Department of Physics, National Taiwan University, Taipei 10617, Taiwan

[‡]Institute of Physics, Academia Sinica, Taipei 11529, Taiwan

[¶]Institute of Atomic and Molecular Sciences, Academia Sinica, Taipei 10617, Taiwan

[∥]National Synchrotron Radiation Research Center, Hsinchu 30076, Taiwan

[⊥]Ministry of Science and Technology, Taiwan Consortium of Emergent Crystalline Materials, Taipei 10622, Taiwan

ABSTRACT: By both experimental measurements and theoretical calculations, we investigated the magnetic and electronic properties of $Li_2Cu(WO_4)_2$ as a tungstate-bridged quasi-one-dimensional (1D) copper spin-(1/2) chain system. Interestingly, magnetic susceptibility $\chi(T)$ and specific heat measurements show that the system undergoes a three-dimensional antiferromagnetic (AF)-like ordering at $T_N \approx 3.7$ K, below a broad $\chi(T)$ maximum at ∼8.9 K indicating a low-dimensional short-range AF spin correlation. Bonner−Fisher model fitting of $\chi(T)$ leads to an AF intrachain exchange constant of $J/k_B = 15.8 \pm 0.1$ K, and mean-field theory estimation gives an interchain coupling constant of $J_\perp/k_B = 1.6$ K, which supports the quasi-1D nature of this spin system. Theoretical evaluation of exchange coupling constants within the generalized gradient approximation (GGA) plus on-site Coulomb interaction (U) shows that the dominant AF exchange interaction is of ∼13.9 K along the *a*-axis with weak interchain coupling, in agreement with the experimental result of a quasi-1D spin-(1/2) chain system. The GGA+U calculations also predict that $Li_2Cu(WO_4)_2$ is a charge transfer-type AF semiconductor with a direct band gap of 1.5 eV.

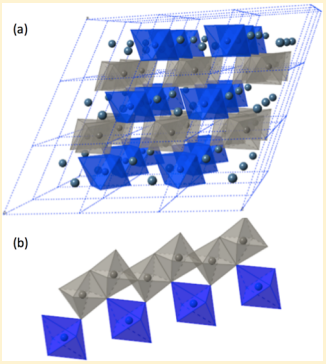

INTRODUCTION

Although one-dimensional (1D) and two-dimensional (2D) Heisenberg antiferromagnetic (AF) spin systems are not expected to exhibit any long-range ordering down to zero K,[1] weak interchain and interplane couplings often lead to various long-range orders at finite temperatures when the thermal energy is comparable to the size of these couplings. In the past decades, therefore, these quasi-low-dimensional spin systems have attracted much attention due to their rich varieties of magnetic ground states. In particular, many low-dimensional Cu spin-(1/2) compounds show exotic magnetic behaviors and ground states including the spin-Peierls transition found in $CuGeO_3$,[2] the gapped ground state in spin ladder system of $SrCu_2O_3$,[3] the Bose−Einstein condensate in $BaCuSi_2O_6$,[4] and many peculiar spin liquid states observed in the Kagome system like $ZnCu_3(OD)_6Cl_2$.[5]

The exotic phases at low temperatures in the low-dimensional materials containing copper spin-(1/2) are controlled by the nature and relative strengths of the spin exchange interactions in them such as geometrical frustration and dimensionality. For example, the different ratios of the AF to ferromagnetic (FM) coupling between the nearest neighbor (NN) and the next-nearest neighbor interactions (NNN) in a quasi-1D $S = (1/2)$ Cu system may lead to different ground states including the FM, AF, incommensurate, and commensurate helical orderings.[6,7]

Intriguingly, quasi-1D magnetic behavior is found in many seemingly three-dimensional (3D) complex copper oxide systems. Most of these quasi-1D cuprates reported in the literature have the superexchange coupling of Cu−O−Cu paths, such as Li_2CuO_2 with edge-sharing CuO_4 plaquettes[8] and Sr_2CuO_3 with corner-sharing CuO_4 plaquettes.[9] In addition, in more complex copper oxides such as $Sr_2Cu(PO_4)_2$ (ref 10), dimerization of CuO_4 plaquettes, which are bridged via corner-sharing PO_4 tetrahedra, has been found to give rise to the so-called supersuperexchange interaction, which results in the quasi-1D magnetic behavior. In $Rb_2Cu_2(MoO_4)_3$ (ref 11), the magnetic interactions have also been found to be dominated by the supersuperexchange interaction involving Cu−O−M−O−Cu with metal (M) polyatomic ionic groups. Clearly, it is of interest to further study complex Cu-based oxides for both novel low-dimensional magnetic phenomena and potentially useful applications.[12,13]

Copper double tungstate $Li_2Cu(WO_4)_2$ has a wolframite-like structure.[14] In $Li_2Cu(WO_4)_2$, all CuO_6 octahedra are linked via corner-sharing with the nonmagnetic edge-sharing zigzag tungstate chains through a Cu−O−W−O−Cu route, as shown in Figure 1. Therefore, the magnetism in $Li_2Cu(WO_4)_2$ would be dominated by the unique supersuperexchange

Received: December 29, 2014
Published: April 13, 2015

ACS Publications © 2015 American Chemical Society

DOI: 10.1021/ic503080e
Inorg. Chem. 2015, 54, 4303−4309

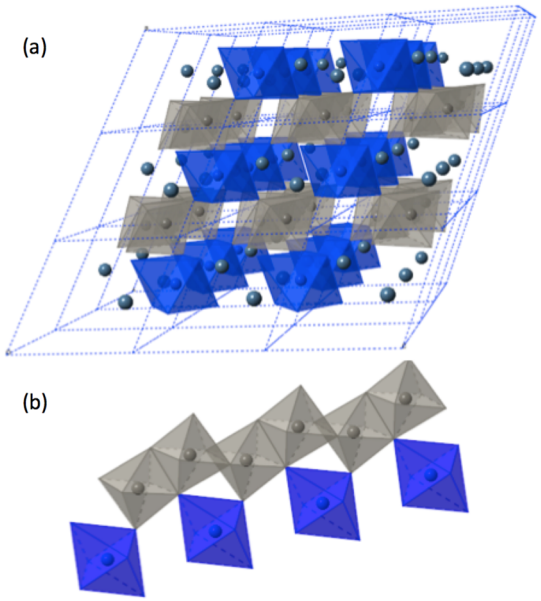

Figure 1. (color online) (a) Crystal structure of $Li_2Cu(WO_4)_2$, where gray and blue octahedra represent CuO_6 and WO_6, respectively. (b) The Cu spin chain is defined by the supersuperexchange route from CuO_6 octahedra which are corner-sharing with the edge-shared nonmagnetic WO_6 zigzag chains along the *a*-direction.

interaction[11] via Cu−O−W−O−Cu paths, which could lead to a number of interesting magnetic phenomena. Nevertheless, apart from the structural characterization,[14] physical properties of $Li_2Cu(WO_4)_2$ have not been investigated. Therefore, we performed magnetic susceptibility and specific heat measurements on $Li_2Cu(WO_4)_2$. Surprisingly, we find that the system does not exhibit spin dimerization at low temperature, although CuO_6 octahedra are arranged in quasi-1D chains. Instead, the system falls to a 3D AF ground state at low temperature. Furthermore, to gain insight into the interesting magnetic behaviors of $Li_2Cu(WO_4)_2$, we also performed a density functional study of the electronic structure and magnetic interactions in this system. Our theoretical calculations corroborate the experimental result that $Li_2Cu(WO_4)_2$ exhibits quasi-1D characteristics and a ground state of 3D AF ordering below $T_N \approx 3.7$ K. Finally, the calculated electronic structure shows that $Li_2Cu(WO_4)_2$ is a direct band gap semiconductor and hence may find applications in optical and magneto-optical devices.

EXPERIMENTAL AND COMPUTATIONAL DETAILS

Polycrystalline $Li_2Cu(WO_4)_2$ sample was prepared by conventional solid-state reaction method. Stoichiometric amounts of high purity (>99.95) CuO, Li_2CO_3, and WO_3 were mixed and ground homogeneously using mortar and pestle. The precursor was heated at 550 °C for 24 h in the air and pressed into pellets to heat at 650 °C for 24 h; single-phase sample can be obtained only after heating at 700 °C for total 160 h in the air with repeated intermediate grindings and pelletizing. The product had a green-yellow color, indicating an optical bandgap of ∼2 eV. High-resolution synchrotron powder X-ray diffraction (XRD) patterns were collected at room temperature (λ = 0.619 Å). The direct current magnetization under zero-field-cooled (ZFC) and field-cooled (FC) conditions was performed with SQUID-VSM (Quantum Design, USA). Heat capacity was measured with a standard relaxation method using PPMS (Quantum Design, USA).

Theoretical calculations have been performed based on density functional theory (DFT) with generalized gradient approximation (GGA).[15] The on-site Coulomb energy *U* has been taken into account using the GGA+U scheme.[16] Since $LiCu_2O_2$ is also a low-dimensional AF oxide with frustrated exchange couplings, and it was found that this U_{eff} value could give rise to an electronic structure of $LiCu_2O_2$ to be in good agreement with the X-ray absorption experiments,[17] we used effective $U_{eff} = (U - J) = 3.6$ eV for the Cu atoms in the GGA+U calculations. We used the accurate full-potential projector-augmented wave (PAW) method[18] as implemented in the Vienna ab initio simulation package (VASP).[19,20] $Li_2Cu(WO_4)_2$ has the triclinic primitive crystal structure (space group $P1^-$, No. 2).[14] The experimental lattice parameters of a = 4.9669 Å, b = 5.4969 Å, and c = 5.8883 Å were used in our calculations. The primitive unit cell of $Li_2Cu(WO_4)_2$ contains one formula unit, that is, it has one Cu atom per unit cell. A (2 × 2 × 2) supercell of various magnetic configurations of copper moments was considered on exploring the magnetic ground state. For the band calculations, the tetrahedron method with Blöchl corrections for the Brillouin zone integration with a Γ-centered Monkhorst−Pack k-point mesh of (8 × 8 × 6) was used. The cutoff energy was taken to be 500 eV, and the convergence criterion for total energy was 1×10^{-6} eV.

RESULTS AND DISCUSSION

Crystal Structure. Figure 2 shows the powder X-ray diffraction (XRD) pattern of $Li_2Cu(WO_4)_2$ obtained with synchrotron X-ray source at room temperature. The XRD pattern of the samples can be indexed with space group $P1^-$ triclinic symmetry. The GSAS Rietveld refinement results summarized in Table 1 are in agreement with those reported in the literature.[14] The edge-sharing WO_6 octahedra form a zigzag

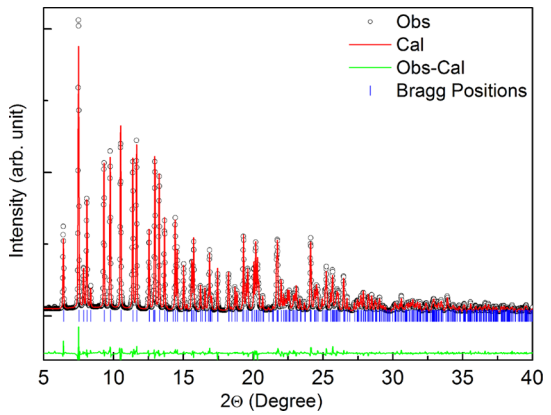

Figure 2. The Rietveld refinement pattern for the powder X-ray diffraction data of $Li_2Cu(WO_4)_2$ using synchrotron X-ray source.

Table 1. List of Parameters Obtained from Rietveld Refinement Results

sample	$Li_2Cu(WO_4)_2$	Cu_x	0.5
crystal structure	triclinic	Cu_y	0.5
space group	$P1^-$	Cu_z	0.0
a (Å)	4.96186(7)	Cu_{Uiso}	0.022(1)
b (Å)	5.49185(9)	Li_x	−0.074(6)
c (Å)	5.88243(9)	Li_y	0.579(5)
V (Å)^3	137.872(4)	Li_z	0.241(5)
α	70.707(1)	Li_{Uiso}	0.0181(4)
β	85.999(1)	Cu−O	2.01(1) × 2
γ	66.041(1)	Cu−O	2.05(1) × 2
W_x	0.2749(2)	Cu−O	2.429(9) × 2
W_y	0.9623(2)		
W_z	0.3381(2)		
W_{Uiso}	0.0181(4)		

DOI: 10.1021/ic503080e
Inorg. Chem. 2015, 54, 4303−4309

chain along the **a**-direction, and the CuO_6 octahedra are corner-shared with the tungstate chain, as illustrated in Figure 1. All CuO_6 octahedra are separated and arranged in 3D, but a clear Cu−O chain through supersuperexchange route can be identified from the relatively shorter inter-Cu distance along the **a**-direction to resemble a quasi-1D chain. The Cu spins are expected to couple through supersuperexchange path of Cu−O−W−O−Cu along the **a**-direction, although weaker inter-chain coupling could also exist along the **b**- and **c**-directions simultaneously, partly due to the bridging zigzag chains of edge-shared pairs of WO_6 along the **a**-direction.

The crystal structure of $Li_2Cu(WO_4)_2$ has a major difference compared to that of $Li_2M(WO_4)_2$ (M = Co and Ni) in the arrangement of WO_4^{2-} polyatomic ion groups; while the WO_6 octahedra in the former form a zigzag chain, edge-shared WO_4 pair of inverted pyramid shape is found in the latter.[14] In addition, the γ angle for $Li_2Cu(WO_4)_2$ is about half of those for $Li_2M(WO_4)_2$ (M = Co and Ni) within the same space group of triclinic symmetry. In particular, the CuO_6 octahedra are significantly elongated ~18%, which could indicate the impact of Jahn−Teller effect when the Cu−O bond length within the basal plane 2.01(0.5)Å is much shorter than that of 2.43(0.01) Å along the apical direction, as summarized in Table 1.

Magnetic Susceptibility. Figure 3 shows the temperature dependence of the magnetic susceptibility $\chi(T)$ measured under applied magnetic field of 1 T in the temperature range between 2 and 300 K. No thermal hysteresis between ZFC and FC curves is observed down to 2 K. A rounded maximum of $\chi(T)$ is found at $T^{\chi}_{max} \approx 8.9$ K, and a sharp drop near ~3.7 K can be identified with the help of its derivative $d(\chi T)/dT$ peak as shown in the inset of Figure 3. The $\chi(T)$ round maximum indicates a typical AF short-range ordering (SRO) for a low-dimensional spin system. The sharp drop of $\chi(T)$ (i.e., the peak of $d(\chi T)/dT$) near ~3.7 K) suggests the onset of a three-dimensional AF-like long-range magnetic ordering (LRO).

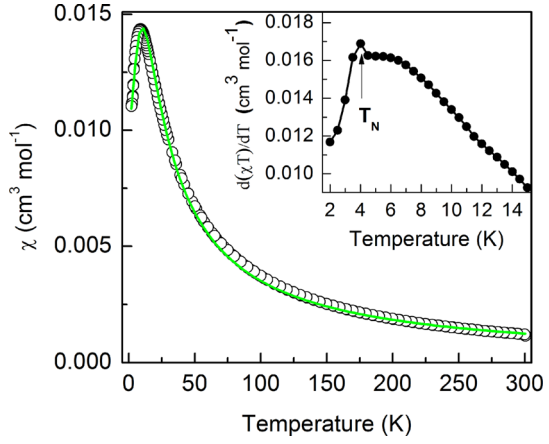

Figure 3. Temperature dependence of magnetic susceptibility for $Li_2Cu(WO_4)_2$ measured under an applied magnetic field of 1 T. χ is fitted with both the Bonner−Fisher model (solid green line) and modified Curie−Weiss law (red dashed line). (inset) The corresponding $d(\chi T)/dT$ at low temperature.

$\chi(T)$ obeys the modified Curie−Weiss law of $\chi(T) = \chi_0 + C/(T - \Theta)$ above ~50 K. The fitting yields Curie constant C = 0.46 cm^3 K/mol, $\chi_0 = -2.5 \times 10^{-4}$ cm^3/mol, and the Weiss temperature $\Theta = -16.3(0.5)$ K. The effective magnetic moment calculated from Curie constant with assumed $g = 2$ is $\mu_{eff} = 1.92\ \mu_B$ per Cu, which is slightly larger than the expected spin-only value of $S = 1/2$ for Cu^{2+} (1.73 μ_B), a g-factor larger than 2 as a result of additional spin−orbit coupling is implied. The negative value of Θ indicates the AF coupling is predominant between Cu^{2+} spins in the paramagnetic regime. The spin frustration ratio $f = |\Theta|/T_N \approx 4.4$ suggests considerable frustration is taking place in the present system.[21]

$\chi(T)$ was also analyzed as an isotropic Heisenberg spin chain using the Bonner−Fisher model for 1D $S = (1/2)$ spin chain system with the nearest neighbor spin AF coupling J as[22]

$$\chi(T) = \frac{Ng^2\mu_B^2}{k_BT} \frac{0.25 + 0.074975x + 0.075236x^2}{1 + 0.9931x + 0.172135x^2 + 0.757825x^3} \quad (1)$$

where $x = |J|/k_BT$. The $\chi(T)$ is fitted satisfactorily in the temperature range of 15−300 K, as shown in Figure 3. The fitted parameters are $J/k_B = 15.8 \pm 0.1$ K and $g = 2.04$. On the other hand, following the mean-field theory approximation, the interchain coupling constant $J_\perp$ for a quasi 1D spin chain system can be estimated by[23]

$$|J_\perp| = \frac{T_N}{4 \times 0.32(\ln(5.8J/T_N))^{1/2}} \quad (2)$$

The interchain interaction $J_\perp/k_B$ is estimated to be ~1.63 K. The ratio between inter- versus intrachain couplings is near ~0.1, which suggests that the spin system could be classified as a quasi-1D system comparing to other quasi-1D spin (1/2) systems reported in the literature for $J_\perp/J \ll 1$.[24−29] In addition, the observed $T^{\chi}_{max} \approx 8.9$ K agrees with the thermodynamic estimation from $T^{\chi}_{max} = 0.640\,85\ J/k_B \approx 10$ K for a quasi-1D (1/2) spin chain satisfactorily.[30]

Figure 4 shows the homogeneous spin susceptibility (M/H) measured under various applied magnetic fields. As the applied field increases, the magnetization values increase slightly below T^{χ}_{max} until nearly saturated at 7 T below $T_N \approx 3.7$ K. The inset of Figure 4 for $d\chi/dT$ reveals that T_N becomes less pronounced and shifts slightly higher with increasing field. Similar increase of T_N with field has been found in various low-dimensional frustrated systems including $BaCdVO(PO_4)_2$ and $Pb_2(VO)(PO_4)_2$,[25,31−33] where T_N increases with higher H initially and decreases toward zero at much higher H. The initial T_N increase could be due to the fact that quantum fluctuation, which competes with the LRO, is suppressed by the magnetic field,

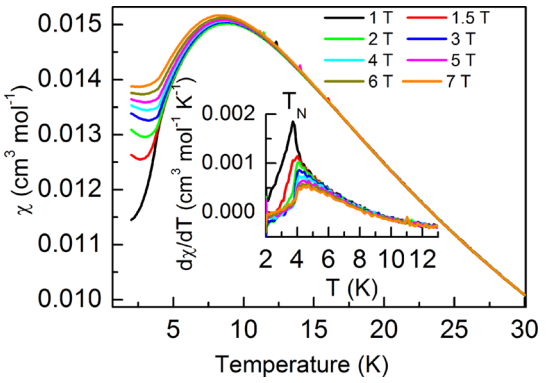

Figure 4. Temperature dependence of the magnetic susceptibility of $Li_2Cu(WO_4)_2$ sample under different applied external fields. (inset) The temperature derivative of magnetic susceptibility $d\chi/dT$.

DOI: 10.1021/ic503080e
Inorg. Chem. 2015, 54, 4303−4309

where external field changes the spin dimensionality from a Heisenberg system to an XY system.[25,34]

The slight upturns of $\chi(T)$ below T_N saturate at high field, which could be attributed to the spin-flop transition of an AF ordering or transformation from a canted AF state to a partially FM state.[35] Figure 5 shows that the magnetization as a function

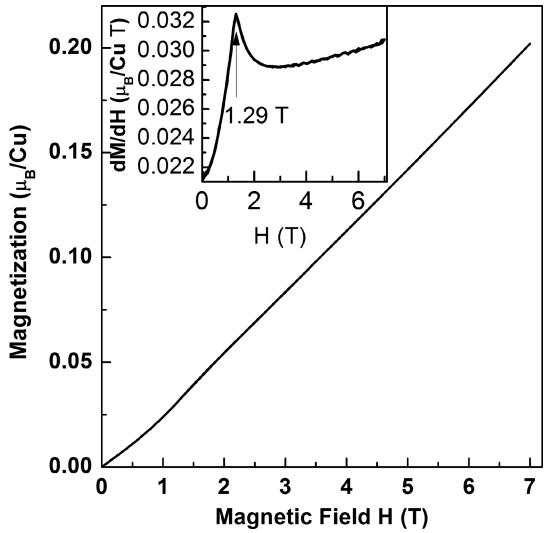

Figure 5. Field dependence of magnetization measured at 2 K. (inset) The derivative magnetization with magnetic field (dM/dH). The susceptibility increases with field until it saturates above a critical field near 1.29 T.

of applied magnetic field at 2 K has a slope variation as revealed by its derivative (dM/dH) shown in the inset. The spin susceptibilities dM/dH at 2 K reveal a rapid nonlinear increase of field dependence but drop and saturate above H = 1.29 T, which suggests a field-induced canted spin reorientation instead of a spin-flop transition, because the spin-flop transition is expected to show higher susceptibility when the field overcomes its on-site spin anisotropy. The relatively small critical field for spin reorientation suggests a weak on-site spin anisotropy for the system, as expected in the weak AF coupling between Cu spins through supersuperexchange route. No hysteresis and remanent magnetization were observed within our experimental limit of 7 T.

Specific Heat. Figure 6a shows the specific heat as a function of temperature in zero magnetic field. C_P shows a broad maximum near $T_{max}^{C_P} \approx 7.5$ K, which is indicative of a crossover from the paramagnetic to an AF short-range spin-correlated state. A λ-shape cusp is observed at ~3.7 K, which provides the concrete evidence for a 3D long-range magnetic ordering following the short-range AF correlation. These two prominent features are qualitatively in agreement with those observed in the magnetic susceptibility shown in Figure 3. Indeed, broad maximum in C_P is expected at $T_{max}^{C_P} = 0.48\ J/k_B$ for the quasi-1D spin (1/2) system.[30] Our $T_{max}^{C_P}$ observation is consistent with the expected value of 7.6 K.

$C_P/T = \alpha + \beta T^2$ was used to fit the C_P data between 14 and 20 K. The fitting yields α = 0.098 J mol^{-1} K^{-2} and $\beta = 5.1 \times 10^{-4}$ J mol^{-1} K^{-4}. The magnetic contribution of specific heat (C_m) is obtained by subtracting the lattice contribution (T^3) term from the total, as shown in Figure 6b. The magnetic entropy (ΔS_m) can be deduced from temperature integration of C_m/T, as shown in Figure 6b. The ΔS_m is saturated to ~5.67 J/

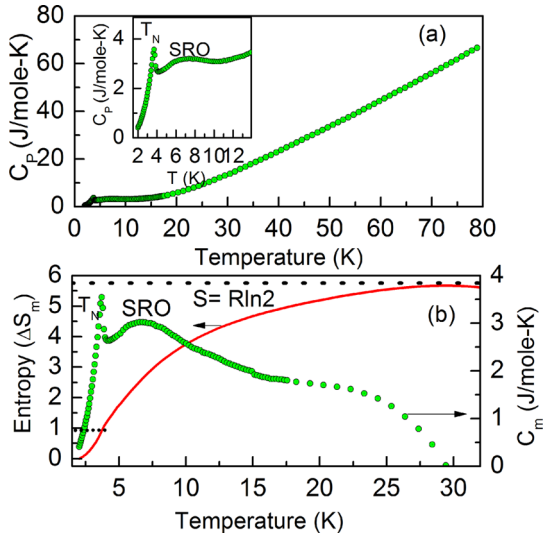

Figure 6. (a) Temperature dependence of specific heat (C_P) of $Li_2Cu(WO_4)_2$ at zero field. (inset) The low-temperature regime. (b) The magnetic entropy (ΔS_m) and C_m vs temperature.

(mol K) at ~30 K, which is very close to the entropy estimated for a spin (1/2) system with $R \times \ln(2S + 1)$ = 5.76 J/(mol K) (R = 8.314 J/mol K). However, the ΔS_m gained at T_N is ~0.96 J/(mol K) to be only ~17% of the total entropy expected, as shown in Figure 6b. Apparently, the rest of magnetic entropy about ~80% is consumed well above T_N. The missing entropy could be related to the short-range magnetic correlation well above T_N;[36] that is, the majority of spin entropy has recovered well above T_N for a low-dimensional system. Indeed, the obtained value of C_m/R at $T_{max}^{C_P}$ is ~0.36 to be in excellent agreement with the expected value of 0.35 for a quasi-1D spin-(1/2) system,[37] as shown in Figure 7. In contrast, C_m/R maximum is expected to be at ~0.44 and ~0.22 for 2D (1/2) square- (non frustrated) and triangular-lattice (frustrated), respectively.[38]

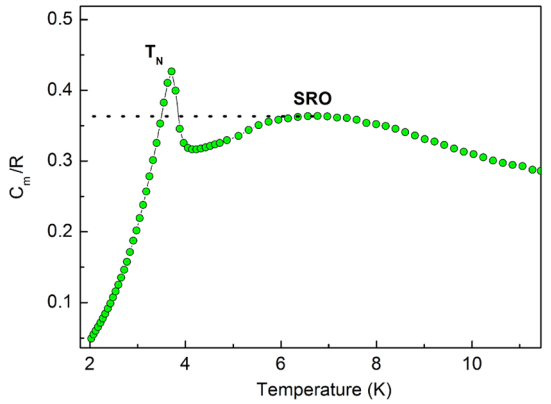

Figure 7. Magnetic contribution of specific heat in unit of gas constant (C_m/R) vs temperature for C_P measured under zero applied magnetic field.

Theoretical Analysis. To find the magnetic ground state of the system, we considered various magnetic configurations possible within the supercell. Of these we selected three configurations, including the overall magnetic ground state of the system for the estimation of exchange interaction parameters J_1, J_2, and J_3 (as shown in Figure 8) along a, b,

DOI: 10.1021/ic503080e
Inorg. Chem. 2015, 54, 4303−4309

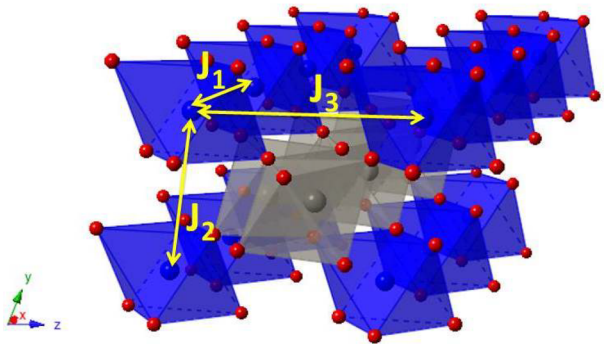

Figure 8. Schematic plot of exchange couplings in $Li_2Cu(WO_4)_2$. Here, Cu, W, and O atoms are represented by blue, gray, and red spheres, respectively.

and *c*-axes, respectively. We label these configurations as A, B, and C. Both FM as well as AF alignments of Cu moments are considered. The calculated total energies of all these configurations are summarized in Table 2. We find that

Table 2. Calculated Total Energy ΔE, Total Magnetic Moment m_s^{tot}, Atomic Moment of Cu m_s^{Cu}, and Band Gap E_g

config	ΔE^a (meV/f.u.)	m_s^{tot} (μ_B/f.u.)	m_s^{Cu} (μ_B/atom)	E_g (eV)
FM	0.0	1.0	0.70	1.28
A	−1.67	0.0	0.70	1.50
B	−1.20	0.0	0.70	1.50
C	−1.53	0.0	0.70	1.45

[a]Relative to the total energy of FM state E_{FM} = −97.2501 eV/f.u.

configuration A has the lowest energy to be the most probable magnetic ground state of the system, where all the NN Cu moments along *a*, *b*, and *c*-axes are antiferromagnetically aligned. We estimated the value of magnetic moment on copper to be 0.7 μ_B, which is slightly off to the 1 μ_B for Cu^{2+}, suggesting that some of the magnetic moments lie outside the approximated spherical radius of copper atom.

In Figure 9 we plotted the band structure (upper) and density of states (lower) of configuration A. We find that the system has an insulating gap of 1.5 eV. On the basis of the atom-resolved density of states, it is quite clear that the valence band is dominated by the oxygen 2p states along with significant contributions from copper 3d and tungsten states, while the conduction band has the dominant contribution from very narrow copper d_{xy} band. Thus, $Li_2Cu(WO_4)_2$ turns out to be an AF charge transfer type insulator with a band gap of 1.5 eV. The magnetic structure is most likely decided by the supersuperexchange coupling primarily between the Cu moments via Cu−O−W−O−Cu path; that is, two CuO_6 octahedra interact through the nonmagnetic WO_6 octahedra.

We evaluated the magnetic exchange coupling J_1, J_2, and J_3 between the nearest-neighbor Cu moments. To evaluate the exchange coupling, we considered the obtained total energy of the supercell of $Li_2Cu(WO_4)_2$ as the sum of the NN spin−spin interactions in terms of the spin Heisenberg model $H = E_0 - \sum_{\langle ij \rangle} J_{ij} \sigma_i \cdot \sigma_j$, where J_{ij} are the exchange interaction parameters between the nearest-neighbor Cu site *i* and site *j*, and σ_i (σ_j) is the unit vector representing the direction of the local magnetic moment at site *i*(*j*). $J < 0$ is assumed for the AF interaction, and

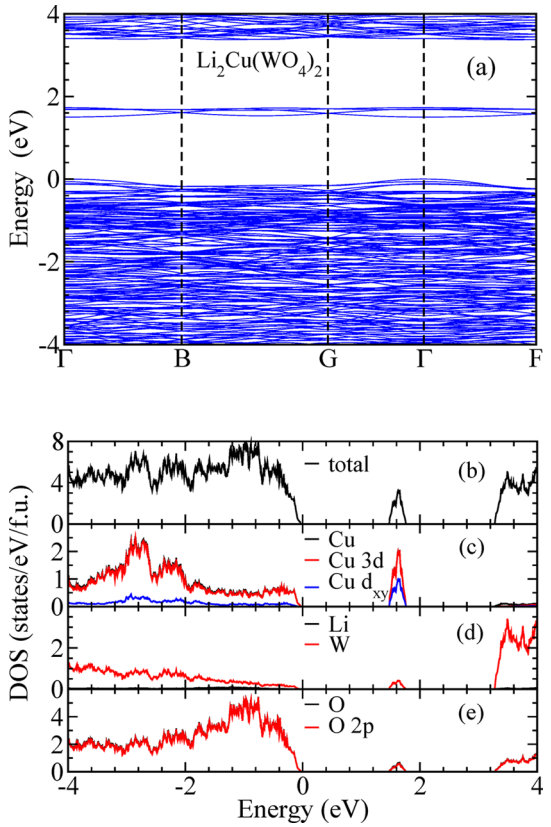

Figure 9. Band structure (upper) and density of states (lower) of configuration A. Top of the valence band was set to zero.

$J > 0$ is assumed for the FM interaction. The constant E_0 contains all spin-independent interactions.

The total energies of the supercell of all considered magnetic configurations are given by $E_{FM} = E_0 - 4J_1 - 4J_2 - 4J_3$, $E_A = E_0 + 4J_1 + 4J_2 + 4J_3$, $E_B = E_0 + 4J_1 - 4J_2 - 4J_3$, and $E_C = E_0 + 4J_1 + 4J_2 - 4J_3$, respectively. Solving the above-mentioned equations we get the values of all exchange interactions listed in Table 3.

Table 3. Calculated Exchange Interaction Parameters J_i (in meV) and Corresponding Cu−Cu Distances d_{Cu-Cu} (in Å) Shown in Figure 8

	J_1	J_2	J_3
J_i	−1.20	−0.33	−0.15
d_{Cu-Cu}	4.967	5.497	5.888

The AF exchange coupling along *a*-axis (J_1/k_B) has the largest magnitude of 13.9 K. This is reasonably close to the experimentally evaluated AF intrachain coupling constant value of 15.8 K. The exchange couplings along *b* and *c*-axes are much smaller compared to the coupling along *a*-axis. $Li_2Cu(WO_4)_2$ can thus be identified as a quasi-1D spin-(1/2) chain. Although each pair of nearest-neighboring CuO_6 octahedra along all three axes in $Li_2Cu(WO_4)_2$ is connected via a pair of nonmagnetic WO_6 octahedra, the exchange coupling along *a*-axis is dominant, which could be due to the strongest bonding of tungsten octahedra with copper octahedra along *a*-axis. Thus, both experimental and theoretical results reveal the quasi-1D character in the present compound.

The 1D nature in $Li_2Cu(WO_4)_2$ is in excellent agreement with supersuperexchange geometrical parameters obtained

DOI: 10.1021/ic503080e
Inorg. Chem. 2015, 54, 4303−4309

Table 4. Supersuperexchange Paths of J_1, J_2, and J_3 and Their Geometrical Parameters

exchange path	distances (Å)				bond angles (deg)		torsion angle (deg)
	Cu−Cu	Cu−O	O···O	O−Cu	Cu−O···O	O···O−Cu	Cu−O···O−Cu
J_1	4.967	2.411	2.589	1.937	90.572	139.86	95.15
J_2	5.496	2.011	2.805	1.937	116.272	150.93	29.51
J_3	5.888	2.011	2.817	2.411	141.344	126.88	30.97

from crystal structure (see Table 4 and Figure 10), which suggest strongest interaction along the *a*-axis. According to Koo et al.[39] the strength of the supersuperexchange interaction depends on the O···O distance and Cu−O−Cu angles mainly, rather than the Cu−Cu distances. When the O···O distance is longer than the van der Waals distance (~2.8 Å), the exchange interaction is negligible.[10] Since the relative distance of O···O is just above the van der Waals distance ~2.8 Å, it is reasonable to find J_2 (O_4−O_2 = 2.805 Å) and J_3 (O_2−O_1 = 2.817 Å) are relatively weak (see Figure 10). On the other hand, the O···O distance is the shortest along the route for J_1 (O_4−O_1 = 2.589 Å), which is in agreement of the strongest AF coupling along the *a*-direction.

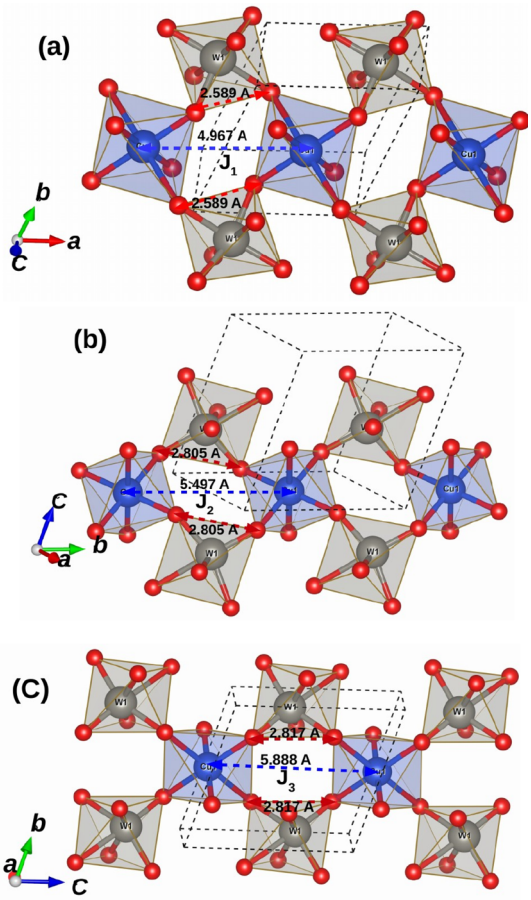

Figure 10. Schematic representations of supersuperexchange interaction paths J_1 (a), J_2 (b), and J_3 (c) between CuO_6 octohedra connected by nonmagnetic WO_6.

CONCLUSIONS

We have performed a joint experimental and theoretical study of the magnetic and electronic properties of $Li_2Cu(WO_4)_2$. Our magnetic susceptibility and specific heat measurements show that $Li_2Cu(WO_4)_2$ exhibits a broad maximum in $\chi(T)$ near ~8.9 K due to a spin SRO, and undergoes an AF LRO below $T_N \approx 3.7$ K. These results suggest that $Li_2Cu(WO_4)_2$ is a quasi-1D (1/2) spin system. Our GGA+U calculations show that the dominant exchange interactions between the copper spins are along the *a*-axis and are mediated via the unique super-superexchange paths through nonmagnetic chains formed by edge-shared WO_6 octahedra. Our GGA+U calculations also predict that $Li_2Cu(WO_4)_2$ is a semiconductor with a direct band gap of 1.5 eV.

AUTHOR INFORMATION

Corresponding Authors

*E-mail: gyguo@phys.ntu.edu.tw. (G.-Y.G.)
*E-mail: fcchou@ntu.edu.tw. (F.-C.C.)

Notes

The authors declare no competing financial interest.

ACKNOWLEDGMENTS

F.-C.C. acknowledges the support provided by MOST-Taiwan under Project No. MOST 102-2119-M-002-004. Financial support for this work from the Academia Sinica Thematic Research Program and the Ministry of Science and Technology of Taiwan is gratefully acknowledged.

REFERENCES

(1) Mermin, N. D.; Wagner, H. *Phys. Rev. Lett.* **1966**, *17*, 1133−1136.
(2) Hase, M.; Terasaki, I.; Uchinokura, K. *Phys. Rev. Lett.* **1993**, *70*, 3651−3654.
(3) Azuma, M.; Hiroi, Z.; Takano, M.; Ishida, K.; Kitaoka, Y. *Phys. Rev. Lett.* **1994**, *73*, 3463−3466.
(4) Giamarchi, T.; Ruegg, C.; Tchernyshyov, O. *Nat. Phys.* **2008**, *4*, 198−204.
(5) Han, T.; Helton, J. S.; Chu, S.; Nocera, D. G.; Rodriguez-Rivera, J. A.; Broholm, C.; Lee, Y. S. *Nature* **2012**, *492*, 406−410.
(6) Wolter, A. U. B.; Lipps, F.; Schapers, M.; Drechsler, S.-L.; Nishimoto, S.; Vogel, R.; Kataev, V.; Buchner, B.; Rosner, H.; Schmitt, M.; Uhlarz, M.; Skourski, Y.; Wosnitza, J.; Sullow, S.; Rule, K. C. *Phys. Rev. B* **2012**, *85*, 014407−16.
(7) Willenberg, B.; Schapers, M.; Rule, K. C.; Sullow, S.; Reehuis, M.; Ryll, H.; Klemke, B.; Kiefer, K.; Schottenhamel, W.; Buchner, B.; Ouladdiaf, B.; Uhlarz, M.; Beyer, R.; Wosnitza, J.; Wolter, A. U. B. *Phys. Rev. Lett.* **2012**, *108*, 117202−5.
(8) Mizuno, Y.; Tohyama, T.; Maekawa, S.; Osafune, T.; Motoyama, N.; Eisaki, H.; Uchida, S. *Phys. Rev. B* **1998**, *57*, 5326−5335.
(9) Kojima, K. M.; Fudamoto, Y.; Larkin, M.; Luke, G. M.; Merrin, J.; Nachumi, B.; Uemura, Y. J.; Motoyama, N.; Eisaki, H.; Uchida, S.; Yamada, K.; Endoh, Y.; Hosoya, S.; Sternlieb, B. J.; Shirane, G. *Phys. Rev. Lett.* **1997**, *78*, 1787−1790.
(10) Salunke, S. S.; Ahsan, M. A. H.; Nath, R.; Mahajan, A. V.; Dasgupta, I. *Phys. Rev. B* **2007**, *76*, 085104−6.
(11) Koo, H. *Inorg. Chem.* **2006**, *45*, 4440−4447.
(12) Kishida, H.; Ono, M.; Miura, K.; Okamoto, H.; Izumi, M.; Manako, T.; Kawasaki, M.; Taguchi, Y.; Tokura, Y.; Tohyama, T.; Tsutsui, K.; Maekawa, S. *Phys. Rev. Lett.* **2001**, *87*, 177401−4.
(13) Ogasawara, T.; Ashida, M.; Motoyama, N.; Eisaki, H.; Uchida, S.; Tokura, Y.; Ghosh, H.; Shukla, A.; Mazumdar, S.; Kuwata-Gonokami, M. *Phys. Rev. Lett.* **2000**, *85*, 2204−2207.

DOI: 10.1021/ic503080e
Inorg. Chem. 2015, 54, 4303−4309

(14) Alvarez-Vega, M.; Rodrguez-Carvajal, J.; Reyes-Cadenas, J. G.; Fuentes, A. F.; Amador, U. *Chem. Mater.* **2001**, *13*, 3871−3875.
(15) Perdew, J. P.; Burke, K.; Ernzerhof, M. *Phys. Rev. Lett.* **1996**, *77*, 3865−3868.
(16) Dudarev, S. L.; Botton, G. A.; Savrasov, S. Y.; Humphreys, C. J.; Sutton, A. P. *Phys. Rev. B* **1998**, *57*, 1505−1509.
(17) Chen, C. L.; Yeh, K. W.; Huang, D. J.; Hsu, F. C.; Lee, Y. C.; Huang, S. W.; Guo, G. Y.; Lin, H.-J.; Rao, S. M.; Wu, M. K. *Phys. Rev. B* **2008**, *78*, 214105−5.
(18) Blöchl, P. E. *Phys. Rev. B* **1994**, *50*, 17953−17979.
(19) Kresse, G.; Hafner, J. *Phys. Rev. B* **1993**, *47*, 558−561; **1994**, *49*, 14251−14269;Kresse, G.; Furthmüller, J. *Comput. Mater. Sci.* **1996**, *6*, 15−50.
(20) Kresse, G.; Joubert, D. *Phys. Rev. B* **1999**, *59*, 1758−1775.
(21) Ramirez, A. P. *Annu. Rev. Mater. Sci.* **1994**, *24*, 453−480.
(22) Bonner, J.; Fisher, M. *Phys. Rev.* **1964**, *135*, A640−A658.
(23) Schulz, H. J. *Phys. Rev. Lett.* **1996**, *77*, 2790−2793.
(24) Savina, Yu.; Bludov, O.; Pashchenko, V.; Gnatchenko, S. L.; Lemmens, P.; Berger, H. *Phys. Rev. B* **2011**, *84*, 104447−8.
(25) Vasilev, A. N.; Ponomarenko, L. A.; Manaka, H.; Yamada, I.; Isobe, M.; Ueda, Y. *Phys. Rev. B* **2001**, *64*, 024419−5.
(26) Vasilev, A. N.; Ponomarenko, L. A.; Smirnov, A. I.; Antipov, E. V.; Velikodny, Y. A.; Isobe, M.; Ueda, Y. *Phys. Rev. B* **1999**, *60*, 3021−3024.
(27) He, Z.; Ueda, Y. *Phys. Rev. B* **2008**, *77*, 052402−4.
(28) Chakhalian, J.; Kiefl, R. F.; Miller, R.; Dunsiger, S. R.; Morris, G.; Kreitzman, S.; MacFarlane, W. A.; Sonier, J.; Eggert, S.; Affleck, I.; Yamada, I. *Phys. B* **2003**, *326*, 422−426.
(29) Baenitz, M.; Geibel, C.; Dischner, M.; Sparn, G.; Steglich, F.; Otto, H. H.; Meibohm, M.; Gippius, A. A. *Phys. Rev. B* **2000**, *62*, 12201−12205.
(30) Johnston, D. C.; Kremer, R. K.; Troyer, M.; Wang, X.; Klumper, A.; Budko, S. L.; Panchula, A. F.; Canfield, P. C. *Phys. Rev. B* **2000**, *61*, 9558−9606.
(31) Nath, R.; Tsirlin, A. A.; Rosner, H.; Geibel, C. *Phys. Rev. B* **2008**, *78*, 064422−7.
(32) Nath, R.; Furukawa, Y.; Borsa, F.; Kaul, E. E.; Baenitz, M.; Geibel, C.; Johnston, D. C. *Phys. Rev.B* **2009**, *80*, 214430−10.
(33) Knafo, W.; Meingast, C.; Inaba, A.; Wolf, Th.; Lohneysen, H. v. *J. Phys.: Condens. Matter* **2008**, *20*, 335208−7.
(34) de Jonge, W. J. M.; Hijmans, J. P. A. M.; Boersma, F.; Schouten, J. C.; Kopinga, K. *Phys. Rev. B* **1978**, *17*, 2922−2925.
(35) Rebello, A.; Smith, M. G.; Neumeier, J. J.; White, B. D.; Yu, Y. K. *Phys. Rev. B* **2013**, *87*, 224427−7.
(36) Schapers, M.; Wolter, A. U. B.; Drechsler, S.-L.; Nishimoto, S.; Muller, K.-H.; Abdel-Hafiez, M.; Schottenhamel, W.; Buchner, B.; Richter, J.; Ouladdiaf, B.; Uhlarz, M.; Beyer, R.; Skourski, Y.; Wosnitza, J.; Rule, K. C.; Ryll, H.; Klemke, B.; Kiefer, K.; Reehuis, M.; Willenberg, B.; Sullow, S. *Phys. Rev. B* **2013**, *88*, 184410−17.
(37) Klumper, A.; Johnston, D. C. *Phys. Rev. Lett.* **2001**, *84*, 4701−4704.
(38) Bernu, B.; Misguich, G. *Phys. Rev. B* **2001**, *63*, 134409−9.
(39) Koo, H.-J.; Dai, D.; Whangbo, M.-H. *Inorg. Chem.* **2005**, *44*, 4359−4365.

DOI: 10.1021/ic503080e
Inorg. Chem. 2015, 54, 4303−4309